Genetic mapping of floral traits associated with reproductive isolation in monkeyflowers (*Mimulus*)

H. D. Bradshaw Jr, S. M. Wilbert*, K. G. Otto & D. W. Schemske†

Center for Urban Horticulture, Box 354115, and * Department of Biochemistry, Box 357350, and † Botany Department, Box 355325, University of Washington, Seattle, Washington 98195, USA

SPECIATION is the process whereby populations acquire sufficient genetic differences to become reproductively isolated[1]. Since Darwin it has been recognized that the tempo and mode of speciation are greatly influenced by the number and magnitude of genetic changes required for reproductive isolation[2–6], but detailed genetic studies have been limited to a few taxa such as *Drosophila*[7]. Genome mapping techniques now widely adopted in plant[8,9] and animal[10,11] breeding make it possible to investigate the genetic basis of reproductive isolating mechanisms in natural populations. Here we use this approach to map eight floral traits in two sympatric monkeyflower species that are reproductively isolated owing to pollinator preference by bumblebees or hummingbirds. For each trait we found at least one quantitative trait locus accounting for more than 25% of the phenotypic variance. This suggests that genes of large effect can contribute to speciation.

Mimulus lewisii (Fig. 1*a*) is bumblebee-pollinated and has pale pink flowers with contrasting yellow nectar guides, a wide corolla opening with forward-thrust petals to provide a landing platform, a small volume of high concentration nectar, and inserted anthers and stigma. *M. cardinalis* (Fig. 1*c*) has typical hummingbird-pollinated flowers, with red petals lacking nectar guides, a narrow tubular corolla, a large volume of nectar, and anthers and stigma exserted to make contact with the hummingbird's forehead. *M. cardinalis* is likely to be derived from a bumblebee-pollinated ancestor[12,13] such as *M. lewisii*. Despite the striking difference in morphology between the two species, they are completely interfertile when artificially mated[14]. The F_1 hybrid (Fig. 1*b*) is vigorous and fertile; when self-pollinated it gives rise to F_2 segregants of astonishing diversity in floral colour and form (Fig. 1*d–i*). Hybrid plants have never been reported in nature in areas of sympatry, despite intensive efforts to find them[14]. As both species flower abundantly and continuously for several months in the late spring and summer when hummingbirds and bumblebees are active, it is clear that differences in floral morphology are sufficient to ensure reproductive isolation. Quantitative trait loci (QTLs) governing floral morphology are thus candidate 'speciation genes'[6].

In conjunction with their work on adaptive genetic variation in natural plant populations, Hiesey *et al.* concluded that most floral characters in the *Mimulus* F_2 are controlled by a 'multiple series of genes rather than by a single gene'[14]. Their genetic inferences were limited, however, by the lack of mendelian markers and linkage maps. We have extended their results by objectively quantifying such variables as flower colour, adding new traits such as nectar volume, and using molecular markers and genome maps to locate QTLs affecting floral traits.

Linkage maps of *M. lewisii* and *M. cardinalis* were constructed (Fig. 2*a*) and used to search for QTLs controlling three classes of floral traits in the F_2: pollinator attraction, reward and efficiency. Traits likely to be involved in pollinator attraction include flower colour, shape and size[15,16]. Pollinator reward was investigated by measuring nectar volume and concentration. Efficiency traits, that is, characters influencing pollen removal and deposition, were stamen and pistil length.

The major floral pigments in the two species are the pink and magenta anthocyanins and the yellow carotenoids[12]. *M. lewisii* petal lobes are pale pink because of a low anthocyanin concentration, and the carotenoids are confined to a pair of yellow nectar guides that extend down the corolla tube (Figs 1*a* and 3*a*, *b*). This pattern of colours is visible to bees and is typical of bee-pollinated flowers[17]. The red colour of *M. cardinalis* flowers results from high concentrations of anthocyanins and carotenoids jointly distributed throughout the petals (Figs 1*c* and 3*a*, *b*). Red flowers are attractive to hummingbirds but outside the colour vision spectrum of bumblebees[17,18]. A QTL on linkage

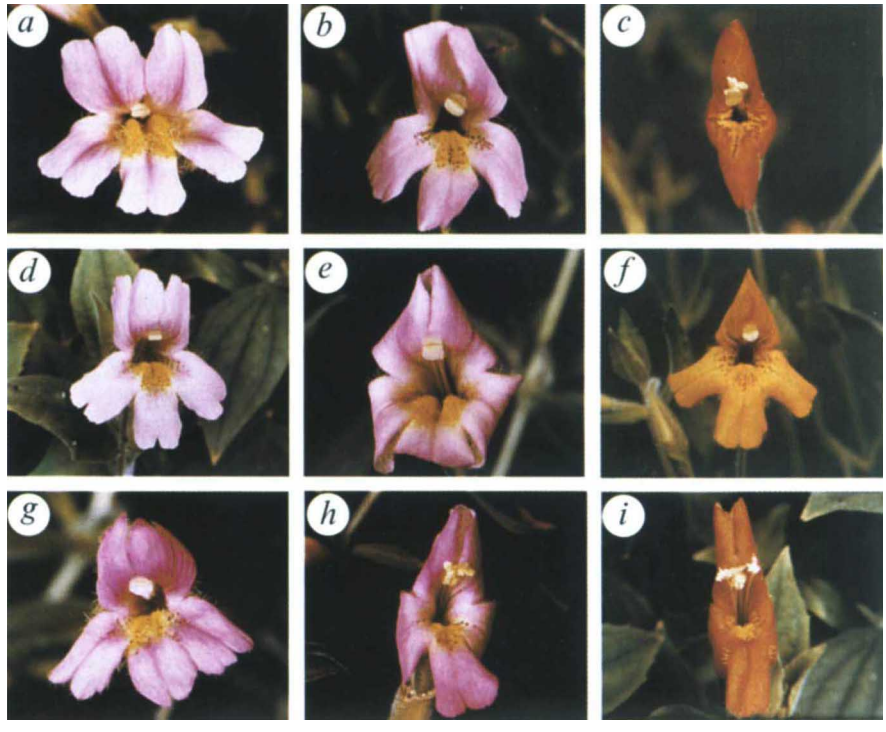

FIG. 1 *Mimulus lewisii* (*a*) was crossed with *M. cardinalis* (*c*) to produce the F_1 (*b*), and a single F_1 plant was self-pollinated to yield the F_2 (*d–i*). *M. lewisii* and *M. cardinalis* seeds (collected in Yosemite National Park, California), were the generous gift of Bob Vickery (University of Utah). The *M. lewisii* seed came from Raisin Lake (seedlot 13357, elevation 2,123 m) and the *M. cardinalis* from Wawona (seedlot 13363, elevation 1,300 m).

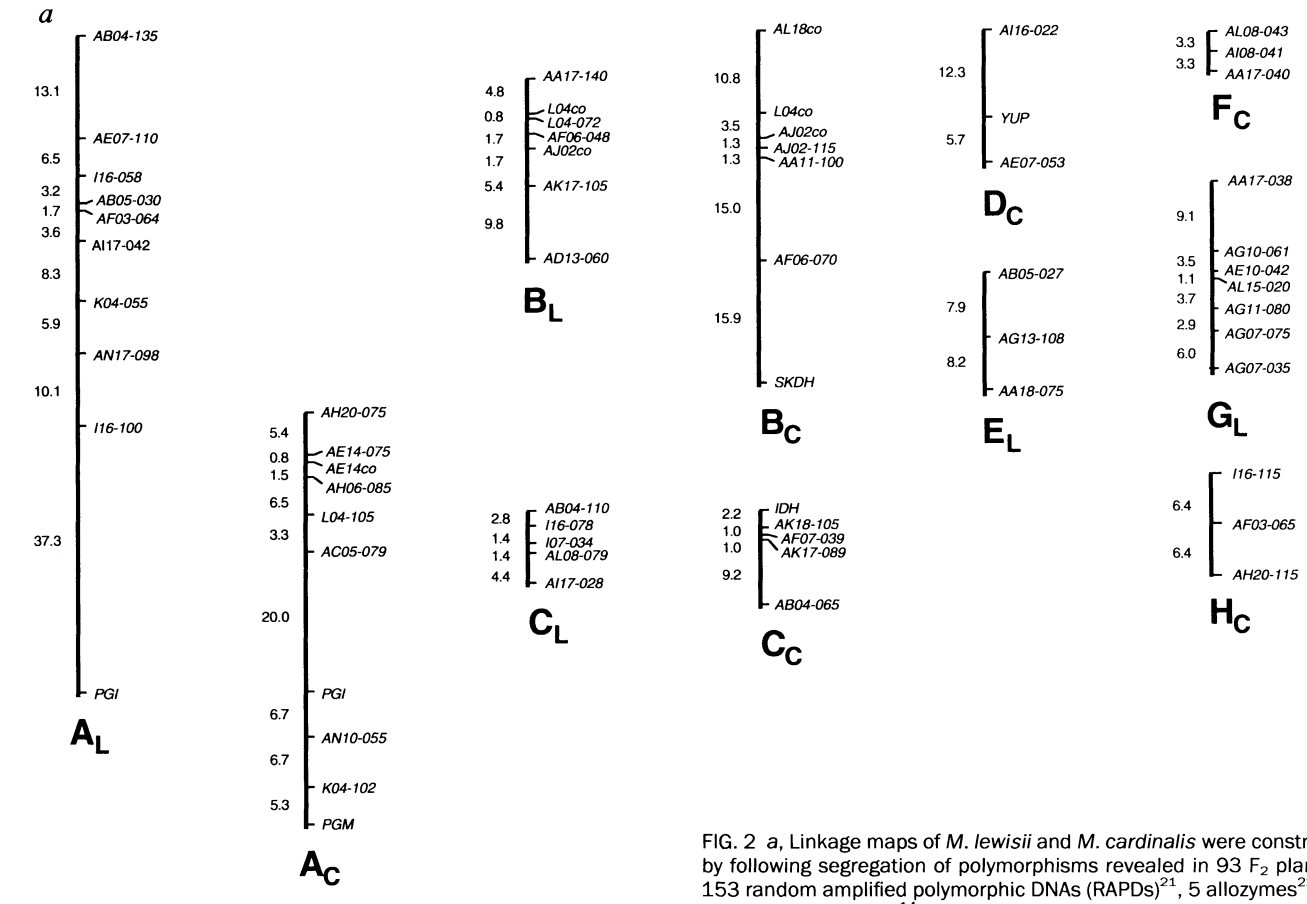

FIG. 2 *a*, Linkage maps of *M. lewisii* and *M. cardinalis* were constructed by following segregation of polymorphisms revealed in 93 F_2 plants by 153 random amplified polymorphic DNAs (RAPDs)[21], 5 allozymes[22], and 1 visible marker (*yup*)[14]. Linkage groups are designated A–H. Subscripts indicate whether the linkage group is derived from the *M. lewisii* (L) or *M. cardinalis* (C) parent. RAPD markers were named according to the primer used and the approximate length of the segregating fragment (for example, AB04-135 is a ~1,350-bp fragment generated by amplification with Operon primer AB4). Haldane map distance (in centimorgans, cM) between markers is shown on the left of each linkage group. As most RAPD markers are inherited in a dominant manner, and dominant markers linked in repulsion are relatively uninformative for linkage mapping in an F_2 (ref. 19), the dominant-marker data were divided into two sets representing segregation of coupling phase markers. Five codominant RAPD markers (for example, AJ02co) and 5 allozyme markers were added to each dataset to help identify homologous linkage groups (for example, linkage group A_L is the *M. lewisii* homologue of A_C from *M. cardinalis*). Maps were constructed using MAPMAKER 3.0 (ref. 23), with a logarithm of the odds ratio (lod) threshold for linkage of 5.0 and a maximum map distance between markers of 25 cM. Only the 59 markers whose linear order is supported by a lod score of $\geqslant 1.3$ are shown. All but 5 markers were detectably linked to one of the eight linkage groups. Segregation distortion ($P<0.01$) from the expected mendelian 3:1 ratio was found at 86/153 RAPD loci (χ^2, d.f. = 1), largely on linkage groups A_L, A_C, D_C, and F_C. *b*, QTL position and magnitude of effect for eight floral traits are shown. Corolla width, petal width, stamen length and pistil length had distributions in the F_2 that were not significantly different ($P<0.05$) from normality (Shapiro–Wilk statistic). Anthocyanin concentration, nectar volume and nectar concentration were square-root-transformed to improve normality; the transformed data were not significantly different from normally distributed. Petal carotenoid concentration could not be transformed to approximate normality. QTLs were located and analysed with MAPMAKER/QTL 1.1 (ref. 8). Lod scores above 2.7 were accepted as significant[24] on the basis of a haploid chromosome number of eight[14], and genetic lengths were estimated[25] as 305 cM for *M. lewisii* and 455 cM for *M. cardinalis*. Permutation tests confirmed that the lod threshold of 2.7 was adequate to exclude spurious assignment of QTLs. Companion QTLs with lod scores >2.0 are shown if the QTL on the homologous linkage group has a lod score >2.7. It is possible that the QTLs we have mapped are composed of two or more linked genes. Fine-structure mapping of individual QTLs in advanced generations of hybrid progeny will be required to resolve this issue[26].

TABLE 1 Location, magnitude of effect, and mode of action for floral QTLs

Class	Trait	Linkage group	Lod	Phen%	Phen mean LL/CC	Dominance*
Attraction	Petal anthocyanin (A_{510})	B_L	3.32	33.5	0.63/0.79	L†
	Petal anthocyanin (A_{510})	B_C	2.69	21.5	0.63/0.74	add†
	Petal carotenoids (A_{450}) ('yellow upper')	D_C	9.59‡	88.3	0.04/0.88	**L**
	Corolla width (mm)	A_C	3.50	25.7	29.3/20.9	add
	Corolla width (mm)	C_L	4.51	68.7	33.2/18.1	add
	Corolla width (mm)	C_C	3.12	33.0	30.4/20.8	add
	Petal width (mm)	B_L	8.14	42.4	10.0/12.5	**C**
	Petal width (mm)	B_C	7.78	41.2	10.1/13.1	C
	Petal width (mm)	H_C	4.27	25.2	11.5/13.3	L
Reward	Nectar volume (μl)	B_L	10.03	48.9	6.9/32.6	**add**†
	Nectar volume (μl)	B_C	10.17	53.1	6.6/32.6	**add**†
	Nectar concentration (Brix%)	B_L	2.83	23.9	31.9/18.7	add†
	Nectar concentration (Brix%)	B_C	3.06	28.5	32.8/18.6	add†
Efficiency	Stamen length (mm)	B_L	4.52	27.7	29.4/34.7	C
	Stamen length (mm)	B_C	4.46	27.5	29.9/35.4	add
	Stamen length (mm)	D_C	3.41	21.3	32.1/37.0	L
	Stamen length (mm)	E_L	2.92	18.7	30.3/34.1	C
	Pistil length (mm)	D_C	5.10	43.9	32.5/40.2	add
	Pistil length (mm)	E_L	6.93	51.9	31.8/39.2	add

Traits were measured as described for Fig. 3 and QTLs were mapped as described in Fig. 2*b* legend. 'Linkage group' refers to the map in Fig. 2*a*; 'Lod' is the maximum lod score for each QTL; 'phen%' is the proportion of phenotypic variance explained by the QTL; and 'phen mean' is the phenotypic mean of F_2 plants homozygous for the *M. lewisii* (LL) or *M. cardinalis* (CC) allele at each QTL. 'Dominance' indicates whether the *M. lewisii* (L) or *M. cardinalis* (C) allele is dominant, or if the mode of QTL action is additive (add). Concordance between estimates of per cent phenotypic variance explained the magnitude of difference between homozygous classes, and mode of QTL action on homologous linkage groups was very good, in spite of the fact that dominant genetic markers provide most of the framework of the maps. The only large discrepancy is for corolla width on linkage group F, which may be explained by the relative lack of informativeness of dominant markers[19] or by violations of the assumption that genetic variance not due to the QTL on F is a random normal variable[20].

* Mode of QTL action is shown in bold if it has a lod support of ⩾1 above competing models of dominance or additivity.

† Mode of QTL action calculation is based on square-root transformation of the phenotypic measurements.

‡ 'Yellow upper' was scored as a qualitative trait, and this lod score is that between *yup* and the nearest linked RAPD marker.

group B explains 21.5–33.5% of the phenotypic variance in extractable anthocyanin (Fig. 2*b*), with the *M. cardinalis* allele having the expected effect of increasing the anthocyanin concentration (Table 1). The presence of carotenoids in the petal lobes is governed by a single locus[14], *yup* (for yellow upper; Fig. 2*a*, *b*), with the *M. cardinalis* allele recessive (Table 1). The existence of *yup* explains the highly skewed distribution of petal carotenoid concentration in the F_2 (Fig. 3*b*).

Two independent QTLs affect corolla width (Fig. 2*b* and Table 1), a measure of the petal reflexing which converts the wide *M. lewisii* flower to a narrow tubular hummingbird flower (Fig. 3*c*). Petal width was included as an indicator of flower size (Fig. 3*d*); two major QTLs were identified (Fig. 2*b* and Table 1).

M. cardinalis produces 80-fold more nectar than *M. lewisii* (40 μl as compared with 0.5 μl per flower; Fig. 3*e*), and half the phenotypic variance in nectar volume in the F_2 is controlled by a single QTL on linkage group B (Fig. 2*b*, and Table 1). The *M. cardinalis* allele increases nectar volume, as expected of a hummingbird-pollinated plant, but simultaneously decreases nectar concentration (Figs 2*b* and 3*f*; Table 1).

M. lewisii and *M. cardinalis* are highly diverged for stamen and pistil length (Fig. 3*g*, *h*). Genetic analysis of stamen and pistil length shows that these traits are partly independent, with a major QTL for stamen length on linkage group B that is not shared with

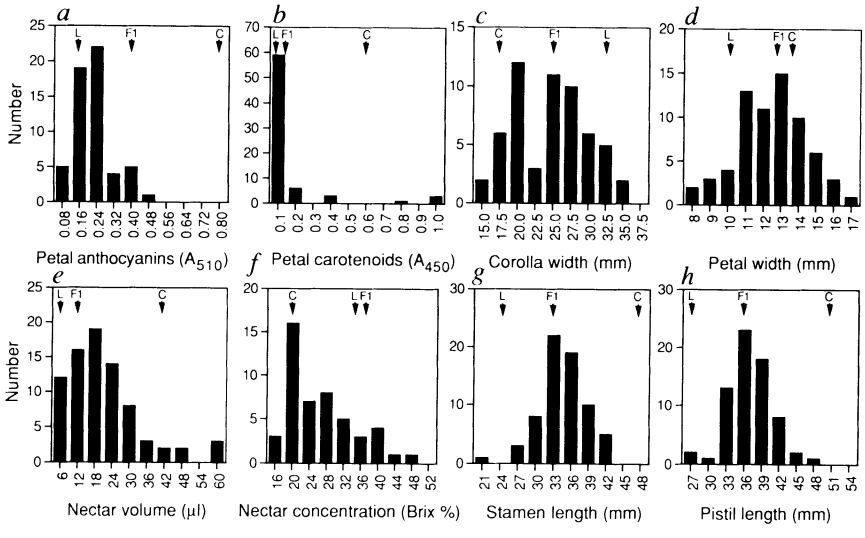

FIG. 3 *a–h*, Distributions of trait values for eight floral characters in the F_2 are shown, along with the mean values for *M. lewisii* (L), *M. cardinalis* (C), and the F_1. Petal anthocyanin concentration was estimated by punching 6-mm disks from the lateral petals of two flowers per plant, extracting the anthocyanins with 0.5 ml methanol/0.1% HCl, and determining the absorbance at 510 nm. Petal carotenoid concentration was estimated similarly, using methylene chloride for extraction and measuring absorbance at 450 nm. The remaining traits were measured on two flowers per plant. Corolla width was measured with the flowers in their natural position across the widest lateral dimension. Petal width was measured on a lateral petal in its natural position. Nectar volume was measured with a graduated pipette tip. Nectar concentration (per cent soluble solids; Brix%) was determined with a hand-held refractometer. Stamen and pistil length were measured with digital calipers from the base of the calyx to the centre of the anther on the longest stamen or to the cleft in the stigma, respectively.

pistil length (Fig. 2*b* and Table 1). Other QTLs for the two traits are shared on linkage groups D_C and E_L (Fig. 2*b*). In every case, the *M. cardinalis* allele increases the length of the stamen or pistil (Table 1).

Our mapping experiments show that for each of eight floral traits likely to play a role in reproductive isolation there is at least one major QTL accounting for more than 25% of the phenotypic variance (Fig. 2*b* and Table 1). This finding suggests that the evolution of reproductive isolation may involve genes of large effect and therefore that speciation may occur rapidly.

The floral syndrome associated with hummingbird pollination is found in 18 families and 39 genera in the flora of western North America, and in many cases has evolved from bee-pollinated ancestors[13]. One plausible scenario for the initial steps in the evolution of hummingbird pollination in *Mimulus* would include a sequence of three major mutations affecting pollinator attraction, reward and efficiency. A mutation at the *yup* locus causes carotenoid pigment deposition throughout the flower, reducing attactiveness to bumblebees by eliminating contrast between the petals and nectar guides. A second mutation at the major 'reward' QTL leads to greatly increased nectar volume and visitation by hummingbirds. A third mutation at the major QTL for pistil length improves the efficiency of pollen deposition by hummingbirds. This hypothesis for the evolution of hummingbird pollination is testable in part by introgressing the *M. cardinalis* allele at each major QTL into a *M. lewisii* genetic background (singly and in combination), followed by assessment of pollinator visitation and its fitness consequences in nature. □

Received 16 March; accepted 28 June 1995.

1. Mayr, E. *Animal Species and Evolution* (Harvard Univ. Press, Cambridge, Massachusetts, 1963).
2. Maynard Smith, J. *A. Rev. Genet.* **17,** 11–25 (1983).
3. Macnair, M. R. & Christie, P. *Heredity* **50,** 295–302 (1983).
4. Barton, N. H. & Charlesworth, B. *A. Rev. Ecol. Syst.* **15,** 133–164 (1984).
5. Gottlieb, L. D. *Am. Nat.* **123,** 681–709 (1984).
6. Coyne, J. A. *Nature* **355,** 511–515 (1992).
7. Coyne, J. A. *Evolution* **47,** 778–788 (1993).
8. Paterson, A. H. *et al. Nature* **335,** 721–726 (1988).
9. Stuber, C. W., Lincoln, S. E., Wolff, D. W., Helentjaris, T. & Lander, E. S. *Genetics* **132,** 823–839 (1992).
10. Andersson, L. *et al. Science* **263,** 1771–1774 (1994).
11. Georges, M. *et al. Genetics* **139,** 907–920 (1995).
12. Vickery, R. K. Jr in *Evolutionary Biology* (eds Hecht, M. K., Steere, W. C. & Wallace, B.) 405–507 (Plenum, New York, 1978).
13. Grant, V. *Proc. natn. Acad. Sci. U.S.A.* **91,** 10407–10411 (1994).
14. Hiesey, W. M., Nobs, M. A. & Bjorkman, O. *Carnegie Inst. Washington Publ. 628* **1,** 1–213 (Washington DC, 1971).
15. Vickery, R. K. Jr *Great Basin Naturalist* **52,** 145–148 (1992).
16. Faegri, K. & van der Pijl, L. *The Principles of Pollination Ecology* (Pergamon, New York, 1979).
17. Daumer, K. *Z. vergl. Physiol.* **41,** 49–110 (1958).
18. Kevan, P. G. in *Handbook of Experimental Pollination Biology* (eds Jones, C. E. & Little, R. J.) 3–30 (Reinhold, New York, 1983).
19. Ott, J. *Analysis of Human Genetic Linkage* (Johns Hopkins Univ. Press, Baltimore, Maryland, 1985).
20. Zeng, Z.-B. *Genetics* **136,** 1457–1468 (1994).
21. Williams, J. G. K., Kubelik, A. R., Livak, K. J., Rafalski, J. A. & Tingey, S. V. *Nucleic Acids Res.* **18,** 6531–6535 (1990).
22. Werth, C. R. *Virginia J. Sci.* **36,** 53–76 (1985).
23. Lander, E. S. *et al. Genomics* **1,** 174–181 (1987).
24. Lander, E. S. & Botstein, D. *Genetics* **121,** 185–199 (1989).
25. Hulbert, S. H. *et al. Genetics* **120,** 947–958 (1988).
26. Paterson, A. H., DeVerna, J. W., Lanini, B. & Tanksley, S. D. *Genetics* **124,** 735–742 (1990).

ACKNOWLEDGEMENTS. We thank R. K. Vickery Jr for seeds and for discussion, J. Doebley for critical review of the manuscript, J. Ramsey, M. Looyenga, M. Booth, Y. Sam and D. Ewing for technical assistance, and M. Gordon and J. Kingsolver for sharing laboratory space and equipment. This work was supported in part by the Royalty Research Fund of the University of Washington.

A reaction–diffusion wave on the skin of the marine angelfish *Pomacanthus*

Shigeru Kondo* & Rihito Asai†

* Kyoto University Centre for Molecular Biology and Genetics, Shogoin-Kawaharacho 53, Sakyo-ku, Kyoto, Japan
† Kyoto University Seto Marine Biological Laboratory, Shirahama-cho, Nishimuro-gun, Wakayama, Japan

In 1952, Turing proposed a hypothetical molecular mechanism, called the reaction–diffusion system[1], which can develop periodic patterns from an initially homogeneous state. Many theoretical models based on reaction–diffusion have been proposed to account for patterning phenomena in morphogenesis[2–4], but, as yet, there is no conclusive experimental evidence for the existence of such a system in the field of biology[5–8]. The marine angelfish, *Pomacanthus*, has stripe patterns which are not fixed in their skin. Unlike mammal skin patterns, which simply enlarge proportionally during their body growth, the stripes of *Pomacanthus* maintain the spaces between the lines by the continuous rearrangement of the patterns. Although the pattern alteration varies depending on the conformation of the stripes, a simulation program based on a Turing system can correctly predict future patterns. The striking similarity between the actual and simulated pattern rearrangement strongly suggests that a reaction–diffusion wave is a viable mechanism for the stripe pattern of *Pomacanthus*.

When juveniles of *Pomacanthus semicirculatus* are smaller than 2 cm long, they have only three dorsoventral stripes (Fig. 1*a*). As they grow, the intervals of the stripes get wider proportionally until the body length reaches 4 cm. At that stage, new stripes emerge between the original stripes (Fig. 1*b*). As a result, all the spaces between the stripes revert to that of the 2-cm juvenile. New lines are thin at first, but gradually get broader. When the body length reaches 8–9 cm, an identical process is repeated (Fig. 1*c*).

The reaction–diffusion system used here consists of two hypothetical molecules (activator and inhibitor) which control the synthesis rate of each other. Fig. 1*d* shows a computer simulation of a reaction–diffusion wave on a growing array of cells. At time 0, the field width is adjusted to be twice the intrinsic wavelength, calculated from the equations used in this simulation. One of the five cells is forced to duplicate periodically. As the field enlarges, all waves widen evenly. When the field length reaches about twice the original length, new peaks appear in the middle of the original peaks, as observed in *P. semicirculatus*, and the wavelength reverts to that of the original.

The juvenile of *P. imperator* has concentric stripes, which increase in number in a manner similar to that of *P. semicirculatus*. But when the *P. imperator* becomes an adult, the stripes become parallel to the anteroposterior axis by a process of continuous cutting and joining of the lines (data not shown). As they grow, the number of lines increases proportionally to body size, and the spaces between the lines are kept at an even width. The stripe pattern of *P. imperator* usually contains several branching points (Fig. 2*a*). During growth, the branching points move horizontally like a zip, resulting in addition of new lines. Figure 2*b–d* shows a branching point moving in the anterior direction until it fuses with the border of the stripe region. In Fig. 2*h–l*, two branching points meet and disappear leaving a new line. This type of rearrangement also happens in the simulation of the reaction–diffusion system, by setting a homologous conformation as a starting pattern (Fig. 2*e–g*, *m–q*). In Fig. 2*e*, the field height is adjusted to be six times the intrinsic wavelength. The waves in the right half are slightly extended, which